

single-particle estimate.<sup>28</sup> These hindrance factors seem rather high, although not unreasonably high, for twice  $K$ -forbidden  $E1$  transitions. No  $M2$  transition from the  $3^+$  to the  $1^-$  level has been observed. The lowest limit can be derived from the capture  $\gamma$ -ray spectrum, Table II. The intensity of the 108.432  $M2$   $\gamma$  ray is less than 0.014%, from which a partial half-life longer than 0.9 sec is derived. The hindrance factor<sup>28</sup> is consequently greater than  $1.2 \times 10^4$  for this once  $K$ -forbidden  $M2$  transition.

<sup>28</sup> A. H. Wapstra, G. J. Nijgh, and R. van Lieshout, *Nuclear Spectroscopy Tables* (North-Holland Publishing Company, Amsterdam, 1959).

From a comparison of the intensities in Tables I and II, one obtains

$$\sigma_1 = (0.58 \pm 0.08) \sigma_T,$$

where  $\sigma_1$  is the partial cross section for the formation of the isomer in the  $(n, \gamma)$  reaction and  $\sigma_T$  is the total capture cross section. The agreement with Brinckmann's<sup>24</sup> value 0.48 is satisfactory.

#### ACKNOWLEDGMENTS

The authors wish to thank Civilingeniør Mogens Olesen and Civilingeniør Per Høy-Christensen for their support in providing the experimental facilities at the Tandem Van de Graaff Laboratory.

### Nuclear Spin and Magnetic Moment of $\text{Ar}^{37}\dagger$

M. M. ROBERTSON\* AND J. E. MACK  
*University of Wisconsin, Madison, Wisconsin*

AND

V. W. COHEN  
*Brookhaven National Laboratory, Upton, New York*

(Received 12 April 1965)

The hyperfine structure of the  $3p^{5/2} - 3p^{5/2}p$  lines of  $\text{Ar}^{37}$  I, studied in an electrodeless discharge, has been used to determine the nuclear spin  $I(\text{Ar}^{37}) = \frac{3}{2}$ , and the nuclear magnetic moment  $\mu(\text{Ar}^{37}) = (-0.95 \pm 0.20)$  nm. The  $\text{Ar}^{37}$ - $\text{Ar}^{40}$  isotope shift, which has been completely resolved for only one line, tends generally to confirm earlier work.

#### EXPERIMENTAL

THE absence of any electronic magnetic moment in the atomic ground state and the small amount of material available make high-resolution optical spectroscopy the most practical means for studying the nuclear moments of  $\text{Ar}^{37}$ .

The  $\text{Ar}^{37}$  was produced by neutron irradiation of optical-quality crystals of  $\text{CaF}_2$ . One sample was irradiated in the Brookhaven graphite reactor and one in the Oak Ridge high-flux reactor; the latter yielded the greater concentration of  $\text{Ar}^{37}$ .

The reaction producing the  $\text{Ar}^{37}$  was  $\text{Ca}^{40} + n \rightarrow \text{Ar}^{37} + \alpha$ . The fluorine underwent the reaction  $\text{F}^{19} + n \rightarrow \text{Ne}^{20} + \beta^-$ , which has a much higher cross section than the  $(n, \alpha)$  reaction. Differential cleanup of Ar in the presence of large quantities of the other gases made it

desirable to separate the Ar from the He and the  $\text{Ne}^{20}$ . The gas purification involved the following steps: heating of the irradiated  $\text{CaF}_2$  in high vacuum to release the trapped gases, adsorption of the  $\text{Ar}^{37}$  on charcoal cooled with liquid nitrogen, pumping off the He and Ne while the  $\text{Ar}^{37}$  remained trapped on the charcoal, compressing the  $\text{Ar}^{37}$  into the quartz electrodeless discharge tube to a pressure of about 3 mm Hg with a modified Toepler pump, and freezing out the Hg vapor with liquid nitrogen while sealing off the discharge tube. We are indebted to Dr. Raymond Davis for essential suggestions and advice in the preparation of the  $\text{Ar}^{37}$ .

The gas-handling system is shown schematically in Fig. 1(a) and the fused-silica electrodeless discharge tube in Fig. 1(b). The tube had a capacity of roughly 0.5 cm<sup>3</sup> and contained about one-half of the total  $\text{Ar}^{37}$  produced. About one-half of the total gas in the tube at first was  $\text{Ar}^{40}$ , whose origin was not determined but which probably came from the atmosphere through the silica while it was hot; the fraction of one per cent of other isotopes would have escaped notice.

The tube was operated submerged in a Dewar with a clear side window. It was excited by a Raytheon 2450-Mc/sec diathermy unit. The high-frequency exci-

† Supported in part by the Research Committee of the Graduate School from funds supplied by the Wisconsin Alumni Research Foundation, by a grant from the National Science Foundation, by the Office of Ordinance Research, and by the U. S. Atomic Energy Commission. This paper substantially comprises the principal part of the 1960 Wisconsin Ph.D. thesis of M. M. Robertson. Microfilm copies of the thesis may be obtained from University Microfilms, 313 North First Street, Ann Arbor, Michigan.

\* Now at Sandia Corporation, Albuquerque, New Mexico.

tation minimized Stark and Zeeman line broadening<sup>1</sup> as well as gas cleanup<sup>2</sup> in the tube.

The observed line breadths were not much greater than the calculated 100°K Doppler breadth, which varied from 13 to 26 mK (where 1 K≡1 cm<sup>-1</sup>, 1 mK = 10<sup>-3</sup> cm<sup>-1</sup>) in the range used, so the observed broadening was attributed principally to Doppler effect.

Spectrograms were made with a Fabry-Perot etalon mounted internally in a glass three-prism spectrograph designed and built at the University of Wisconsin by George Streater. Depending upon the structure being investigated, spacers from 5 to 50 mm were used, yielding resolutions up to a little more than 10<sup>6</sup>. The 60-mm quartz interferometer plates were flat to about one twenty-fifth of a wavelength of green light. Multi-layer dielectric coatings of ZnS and cryolite with over 90% reflectance over intervals of about 1000 Å were used for most of the work. Silver coatings were also used; they were usable over wider wavelength ranges but they suffered greater absorption losses and deteriorated rather rapidly. Three pairs of dielectric-coated plates were used, with reflectance peaks at about 8125, 5600, and 4300 Å. The prisms of the spectrograph had high dispersion in the red. Cameras with focal lengths of 55 and 125 cm were used. Spectrograms were also taken on the Argonne National Laboratory's 9-m Paschen-Runge spectrograph, made available through the courtesy of F. S. Tomkins and M. Fred. This instrument was used in the third order at a theoretical resolution of 315 000, which, however, turned out to be insufficient to resolve any of the line structures under investigation.

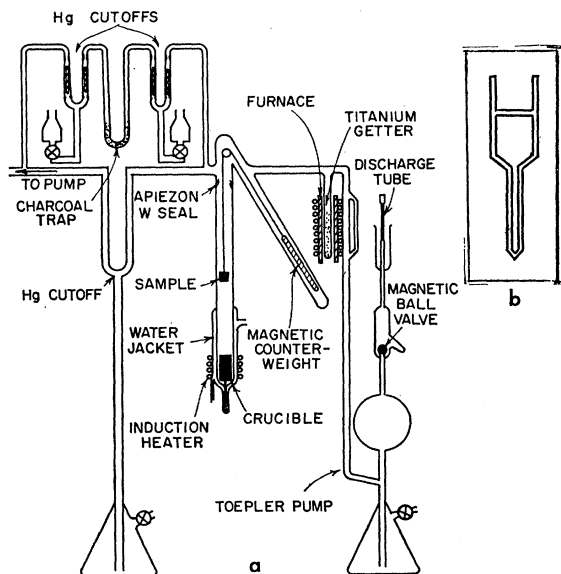


FIG. 1. (a) The gas-handling and purifying system, cross section (schematic); (b) the electrodeless discharge tube.

<sup>1</sup> R. A. Sawyer, *Experimental Spectroscopy* (Prentice-Hall Inc., Englewood Cliffs, New Jersey, 1951), 2nd ed., p. 28.

<sup>2</sup> E. Jacobsen and G. R. Harrison, *J. Opt. Soc. Am.* **39**, 1054 (1949).

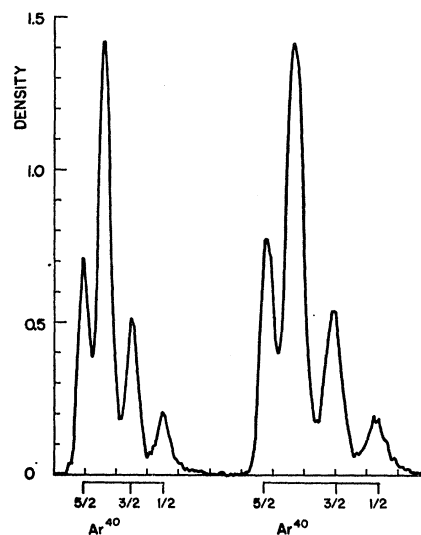


FIG. 2. Microdensitometer trace (retraced) of two orders of the "Ar<sup>37</sup>" 12 578 K, 7948 Å line,  $3p^5(\frac{3}{2})4s[\frac{1}{2}]0^{\circ}-3p^5(\frac{3}{2})4p[\frac{3}{2}]_1$ , from a Fabry-Perot with a 2.00-cm spacer (free spectral range, 250 mK). The strongest component is due to Ar<sup>40</sup>. The other three components, in order of decreasing strength, arise from the  $F=\frac{5}{2}, \frac{3}{2}$ , and  $\frac{1}{2}$  transitions, respectively, as indicated, of the  $J=1$  level. The evenly spaced abscissa marks are position scale points, randomly placed relative to the (nonlinear) wave-number scale.

Altogether, about 100 spectrograms were made, with Eastman emulsions I-N, IV-N, 103a-F, and 103a-O. Photometric calibration was accomplished under standard development procedures by exposure through a calibrated Kodak optical density wedge.

Exposure times varied from 1 sec to 15 min. The shortness of the exposures obviated the necessity of extra precautions against temperature and barometric pressure changes. The source-tube pressure would become so low after about 6 h of operation that the tube would have to be heated to release the argon from the walls and each heating further impaired the optical quality of the tube.

The Ar<sup>40</sup> components in the patterns were positively identified by taking successive narrow-slit etalon exposures of an "Ar<sup>37</sup>" (really a 37-40 mixture) tube and an Ar<sup>40</sup> tube in a special plate holder, with the spectrographic plate moved slightly in the direction of the dispersion between exposures.

Although the Ar<sup>40</sup> contaminant in the Ar<sup>37</sup> tube initially comprised about half the argon in the tube, the percentage increased day by day from the decay of Ar<sup>37</sup> to Cl<sup>37</sup>. The Cl<sup>37</sup> did not appear in the spectrograms. After seven Ar<sup>37</sup> half-lives, even an extremely overexposed spectrogram of the "Ar<sup>37</sup>" tube showed only the Ar<sup>40</sup> component.

The fringe system was centered along the length of the spectrum lines and the ring diameters could be measured out as far as 6 to 12 orders of interference, depending upon the spacer used. Figure 2 displays two orders of the only completely resolved line. Most of the measurements were made to a precision of about 2 μ

TABLE I. Line patterns and level hyperfine structure and isotope shift.

	$3p^5(\frac{3}{2})4s[\frac{3}{2}]_2^{\circ}$ "1s <sub>5</sub> ; <sup>2</sup> P <sub>2</sub> " 93 143.800	$3p^5(\frac{3}{2})4s[\frac{3}{2}]_1^{\circ}$ "1s <sub>4</sub> ; <sup>2</sup> P <sub>1</sub> " 93 750.639	$3p^5(\frac{3}{2})4s[\frac{3}{2}]_0^{\circ}$ "1s <sub>3</sub> ; <sup>2</sup> P <sub>0</sub> " 94 553.707	$3p^5(\frac{3}{2})4s[\frac{3}{2}]_1^{\circ}$ "1s <sub>2</sub> ; <sup>1</sup> P <sub>1</sub> " 95 399.870	A or ( $\sigma - \sigma_{40}$ ) <sub>F</sub> IS(mass) This paper.
$3p^5(\frac{3}{2})4p[\frac{3}{2}]_1$ "2p <sub>10</sub> " 104 102.144	-45.5' +17.5 mK 9123 Å, 10 958 K	...	...	...	A = +7 mK IS(25.60) 24 mK
$3p^5(\frac{3}{2})4p[\frac{3}{2}]_2$ "2p <sub>9</sub> " 105 462.804	-53 to +27 8115 Å, 12 319 K	...	...	...	A = +5 mK IS(24.09) 24 mK
$3p^5(\frac{3}{2})4p[\frac{3}{2}]_2$ "2p <sub>8</sub> " 105 617.315	-47.5' (-23.9) (+29.3) +36.8 8014 Å, 12 473 K	-48 to 0 8424 Å, 11 866 K	...	9784 Å	A = +4 mK IS(23.92) 23 mK
$3p^5(\frac{3}{2})4p[\frac{3}{2}]_1$ "2p <sub>7</sub> " 106 087.305	...	-53 to +35 8103 Å, 12 336 K	-54.8 -25.6' +15.2'' 8667 Å, 11 533 K	...	A = +18 mK IS(23.40) 21 mK
$3p^5(\frac{3}{2})4p[\frac{3}{2}]_2$ "2p <sub>6</sub> " 106 237.597	-58.3 -30.9'' +31.4' 7635 Å, 13 093 K	...	...	9224 Å	A = +7 mK IS(23.23) 24 mK
$3p^5(\frac{3}{2})4p[\frac{3}{2}]_0$ "2p <sub>5</sub> " 107 054.319	...	-43.9' +30.2 7514 Å, 13 303 K	...	...	+23 <sub>3/2</sub> IS(22.32) 23 mK
$3p^5(\frac{3}{2})4p[\frac{3}{2}]_1$ "2p <sub>4</sub> " 107 131.755	-37'' +27' +53 7147 Å, 13 988 K	...	-81.5 -39.7' +32.7'' 7948 Å, 12 578 K	-112 -42.0'' +54.0' 8521 Å, 11 731 K	-49.5 <sub>1/2</sub> -7.7 <sub>3/2</sub> +64.7 <sub>5/2</sub> IS(22.23) 21.5 mK
$3p^5(\frac{3}{2})4p[\frac{3}{2}]_2$ "2p <sub>3</sub> " 107 289.747	-48 to +41 7067 Å, 14 145 K	-56.9 7384 Å, 13 539 K	...	-91.3 -31.6'' +19.9' 8408 Å, 11 889 K	A = +17 mK IS(22.06) 21 mK
$3p^5(\frac{3}{2})4p[\frac{3}{2}]_1$ "2p <sub>2</sub> " 107 496.463	-69.0'' +42.5' +67.8 6965 Å, 14 353 K	-50.6' +33.4 7272 Å, 13 745 K	...	-88.6'' +29.8 +88.8' 8264 Å, 12 096 K	A = -8 mK IS(21.23) 23 mK
$3p^5(\frac{3}{2})4p[\frac{3}{2}]_0$ "2p <sub>1</sub> " 108 722.668	...	...	...	-86.0' +76.1 7503 Å, 13 322 K	+23 <sub>3/2</sub> IS(20.46) 23 mK
$3p^5(\frac{3}{2})5p[\frac{3}{2}]_0$ "3p <sub>5</sub> " 117 563.020	...	...	...	-94.1' +65.1 4510 Å, 22 163 K	+11 <sub>3/2</sub> IS(10.62) 11 mK
A or ( $\sigma - \sigma_{40}$ ) <sub>F</sub> IS(mass) This paper.	A = +15 mK IS(37.80) 35 mK	A = +19 mK IS(37.13) 39 mK	+32.0 <sub>3/2</sub> IS(36.23) 32.0 mK	A = +40.3 mK IS(35.29) 44.5 mK	

with a Gaertner traveling microscope mounted on a special base. In most instances lines were measured three times per plate and on at least three different plates. Measurement of the inherently asymmetric inner fringes was sometimes omitted. The data were reduced by procedures similar to those described by Meissner.<sup>3</sup> We are indebted to Hugo Tscharnack for help in the measurement and interpretation of the plates.

#### HYPERFINE STRUCTURE, I, AND $\nu$

Table I shows the patterns found in the lines studied and the Ar<sup>37</sup> hyperfine structure deduced and the Ar<sup>37</sup>-Ar<sup>40</sup> shift found or generally confirmed therefrom.

At the head of each row and column is the symbol and the value of an energy level: an odd  $3p^54s$  level for each column and an even  $3p^54p$  (or in one case  $3p^55p$ ) level for each row. In the upper half of each heading box, Racah  $jl$  or pair notation is used for the level:  $3p^5(j)nl[K]_J$ , where  $j$  is the angular momentum of the  $3p^5$  core,  $K$  is the resultant of  $j$  and the orbital angular momentum  $l$  of the excited electron, and the total angular momentum  $J$  is the resultant of  $K$  and the loosely-coupled spin  $\frac{1}{2}$  of the excited electron. In the lower half there appears in quotation marks the Paschen symbol for the level in which the subscript is arbitrary and not indicative of  $J$  value like modern subscripts, and for the odd levels an  $LS$ -coupling symbol. Outside

the quotation marks is the energy value for the Ar<sup>40</sup> level.<sup>4</sup>

In each square of the main part of the table there appears in the upper half a list of the positions of the components other than the Ar<sup>40</sup> component found in the line, expressed in millikaysers with respect to the Ar<sup>40</sup> component as zero. The strongest listed component is indicated by a prime (') except that when three relative intensities are shown, the strongest is shown with a double prime (") and the second strongest with a single prime. In a few instances a range of blackening is indicated by numbers joined by the word "to." In the lower half appears the approximate wavelength in angstroms (Å) and the wave number in kaysers (K). A row of three dots in a square indicates a permitted line that has not been measured.

At the foot of each column and row, there is shown in the upper half, wherever possible, each hfs sublevel in mK (referred to the Ar<sup>40</sup> level, with one Ar<sup>40</sup> level arbitrarily placed) with its  $F$  value as a subscript, otherwise the hfs interval factor  $A$  for the level; and in the lower half, the simple isotopic mass shift calculated from recent data of Koenig *et al.*,<sup>5</sup> in parentheses, followed by the isotope shift observed in this work (see the second paragraph below) or presumed from the work of Meyer.<sup>6</sup>

<sup>4</sup> C. E. Moore, Natl. Bur. Std. (U. S.) Circ. 467 (1949), Vol. 1, p. 212.

<sup>5</sup> L. A. König, J. H. E. Mattauch, and A. H. Wapstra, Nucl. Phys. 31, 18 (1962).

<sup>6</sup> H. Meyer, Helv. Phys. Acta 26, 811 (1953).

<sup>3</sup> K. W. Meissner, J. Opt. Soc. Am. 31, 405 (1941); 32, 185 (1942); 32, 211(E) (1942).

Only in one line,  $3p^5(\frac{1}{2})4s[\frac{1}{2}]_0^0 - 3p^5(\frac{1}{2})4p[\frac{3}{2}]_1$  at 12578 K, (cf. Fig. 2) with four clearly resolved components, was the Ar<sup>37</sup> structure, which in this case can have no more than three components, unquestionably completely resolved itself and resolved from the simple Ar<sup>40</sup> line. The measured interval ratio  $1.73 \pm 0.06$  was to be compared with the following values of  $(I+1)/I$ , computed for nuclei free from higher moments:  $I = \frac{1}{2}$  (only one interval, no ratio);  $I = \frac{3}{2}$ , 1.67;  $I = \frac{5}{2}$ , 1.40;  $I > \frac{5}{2}$ ,  $< 1.3$ . The extraordinarily large higher moments that would have been needed to produce the observed interval ratio with any  $I$  greater than  $\frac{3}{2}$  would have caused a wide variation in interval ratio among other lines, which is not observed. Therefore we consider it definitely established that  $I(\text{Ar}^{37}) = \frac{3}{2}$ . Estimates and microphotometer observations of the relative intensities tend to confirm the  $I$ -value.

Only in the case of the one completely resolved line was the isotope-shift measurement taken to be independently authoritative. In all other cases there was at least some weight given to Meyer's<sup>6</sup> work; nowhere was there any serious discrepancy with that work.

The hfs multiplets are all in the normal order except that for  $3p^5(\frac{1}{2})4p[\frac{1}{2}]_1$ , which is inverted; similar results have been reported in Xe<sup>129</sup> and Xe<sup>131</sup> by Bohr, Koch, and Rasmussen<sup>7</sup> and in Kr<sup>83</sup> by Bayer-Helms.<sup>8</sup>

The magnetic moment was calculated by using the Fermi-Segré<sup>9</sup> and Goudsmit<sup>10</sup> relationships with the individual electron  $a$ -factors derived according to the method of Breit and Wills<sup>11</sup> for an  $sp$  configuration modified in accordance with the fact that the core is really not  $p$  but  $-p$ . This method relates the individual electron interval factors to the measured interval factor of the level, taking account of the wave-function mixing in cases where different states have the same  $J$  value. Calculation was feasible only in the case of the  $3p^54s$  configuration.<sup>12</sup> With the aid of the derived relationship  $a(p_{3/2}) = 0.197a(p_{1/2})$ , the calculation yields

$$\begin{aligned} A\{3p^5(\frac{3}{2})4s[\frac{3}{2}]_2\} &= 0.25000a(4s) + 0.14775a(3p_{1/2}), \\ A\{3p^5(\frac{3}{2})4s[\frac{3}{2}]_1\} &= -0.08438a(4s) + 0.26616a(3p_{1/2}), \\ A\{3p^5(\frac{1}{2})4s[\frac{1}{2}]_1\} &= 0.33438a(4s) + 0.48010a(3p_{1/2}). \end{aligned}$$

<sup>7</sup> A. Bohr, J. Koch, and E. Rasmussen, *Arkiv Fysik* **4**, 455 (1952).

<sup>8</sup> F. Bayer-Helms, *Z. Physik* **154**, 175 (1959).

<sup>9</sup> E. Fermi and E. Segré, *Z. Physik* **82**, 729 (1933).

<sup>10</sup> S. Goudsmit, *Phys. Rev.* **43**, 636 (1933).

<sup>11</sup> G. Breit and L. A. Wills, *Phys. Rev.* **44**, 470 (1933).

<sup>12</sup> Further details may be found in the thesis cited in the footnote to the title.

The coefficients in the last two of these equations were computed from the fine structure of the  $3p4s$  configuration.

One may compute the following relations between the nuclear magnetic moment  $\mu$  (in nuclear magnetons) and the  $a$ 's (in mK):

$$\mu = 0.03497Ia(4s) = 0.009965Ia(4p_{1/2}).$$

The  $A$ 's of the three split  $3p^54s$  levels give redundant values for the  $a$ 's and consequently for  $\mu$ , which can be computed respectively from the first and second, first and third, and second and third levels, as follows:

$$\begin{array}{ll} a(4s) = 15.0 \text{ mK}, & \mu = 0.79 \text{ nm}; \\ & 17.7 \quad 0.93 \\ & 12.4 \quad 0.65 \\ \text{Mean: from } a(4s), & \mu = 0.79 \text{ nm}; \\ a(3p_{1/2}) = 76.1 \text{ mK}, & \mu = 1.14 \text{ nm} \\ & 71.6 \quad 1.07 \\ & 75.3 \quad 1.13 \\ \text{Mean: from } a(3p_{1/2}), & \mu = 1.11 \text{ nm}. \end{array}$$

Although the spread of  $\mu$  computed from either  $a$  is not very large, the discrepancy between the calculations from the two  $\mu$ 's is considerable, as usually turns out to be the case. Balancing the greater confidence usually accorded to  $s$ -electron computations against the tighter binding of the  $p$ -electron hole in this case, we have weighted the values equally and made what is believed to be a conservative estimate of error in arriving at the final value<sup>13</sup>

$$\mu(\text{Ar}^{37}) = (0.95 \pm 0.20) \text{ nm}.$$

The nuclear moments found,  $I = \frac{3}{2}$  and  $\mu$  near the upper Schmidt line  $\mu(d_{3/2})$  value of 1.15, are just what is expected according to the shell model, which predicts the quantum numbers  $1d_{3/2}$  for the nineteenth neutron.<sup>14</sup>

#### ACKNOWLEDGMENT

We are greatly indebted to O. S. Duffendack for his participation in this project during the prolonged absence of one of the authors.

<sup>13</sup> This value differs somewhat from that referred to in the work cited in footnote 12 on account of a critical re-evaluation of the data, involving some small changes in Table II and increased confidence in the result.

<sup>14</sup> M. G. Mayer and J. H. D. Jensen, *Elementary Theory of Nuclear Shell Structure* (John Wiley & Sons, New York, 1955), p. 83.